INNOVATIVE TECHNOLOGICA
METHODICAL RESEARCH JOURNAL
ISSN: 2776-0987 Volume 2, Issue 11, Nov., 2021

DESTRUCTION OF SOIL CRUST BY IMPULSE IMPACT OF SHOCK WAVE AND GAS-DYNAMIC FLOW OF DETONATION PRODUCTS

Rasuljon Tojiyev
Professor of Fergana Polytechnic Institute, Fergana, Republic of Uzbekistan
E-mail: r.tojiyev@ferpi.uz, orcid-0000-0001-5636-5840

Nargiza Rajabova
Assistant, Fergana Polytechnic Institute, Fergana, Republic of Uzbekistan
E-mail: n.rajabova@ferpi.uz, ORCID:0000-0001-7648-4468

Bobojon Ortiqaliyev
Assistant, Fergana Polytechnic Institute, Fergana, Republic of Uzbekistan
E-mail: b.ortiqaliyev@ferpi.uz, ORCID:0000-0002-7270-749X

Malika Abduolimova
Assistant, Fergana Polytechnic Institute, Fergana, Republic of Uzbekistan
E-mail: m.abduolimova@gmail.com

Abstract
The article discusses the filming of the process of destruction of the soil crust with visualizations of the shock wave movement from the cut of the GDV (generator of detonation waves) to the soil crust and with the visualization of deformation and fragmentation of the crust during its destruction.

Keywords: Survey, process, soil crust, cylinder, generator, ignition chamber, valve, sensor, turbulator, pipe, collector.

Introduction

Objective of the study: shooting the process of destruction of the soil crust with visualization of the shock wave movement from the cut of the GDV (generator of detonation waves) to the soil crust and visualization of deformation and fragmentation of the crust during its destruction [1-7].

The destruction of the soil crust was achieved by the impulse action of a shock wave and a gas-dynamic flow of detonation products generated by the working body of the

INNOVATIVE TECHNOLOGICA
METHODICAL RESEARCH JOURNAL
ISSN: 2776-0987 Volume 2, Issue 11, Nov., 2021

detonation wave generator (GDW). The studies were carried out according to the scheme with a connected gas outlet on fuel-air mixtures. GDV was selected with the condition of complete imitation of one working body developed for the introduction of a real gas-dynamic soil cultivator – GDRP [8-13]. The GDV generator (Fig. 3.11) includes an ignition chamber (1) with a check valve assembly (2) and a spark plug (3), sections (4), a tabulator (5), a booster pipe (6), LH-608 sensors (7) and outlet nozzle (8).

The source of the thermal-air mixture (FA) was V-shaped, eight-cylinder, four-stroke carburetor engine of the ZIL-131 car with minor changes to the ignition system and the gas exhaust system [14-17].

Figure 1. the scheme of operation of the fuel assembly source is presented. Engine cylinders 1,2,3,4 (right group) operate in normal mode with ignition of the mixture from the engine ignition system and drive the crankshaft into rotation. Cylinders 5,6,7,8 (left group) with the ignition off are displaced into the exhaust manifold, which unites these cylinders, the fuel-air mixture, which is fed to the GDV via a flexible hose [18-20].

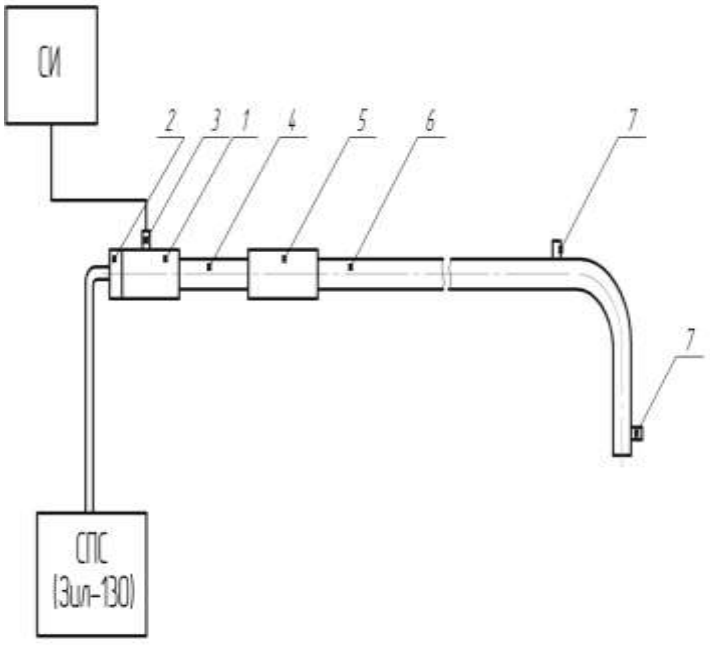

Fig. 1. GDV scheme

INNOVATIVE TECHNOLOGICA
METHODICAL RESEARCH JOURNAL
ISSN: 2776-0987 Volume 2, Issue 11, Nov., 2021

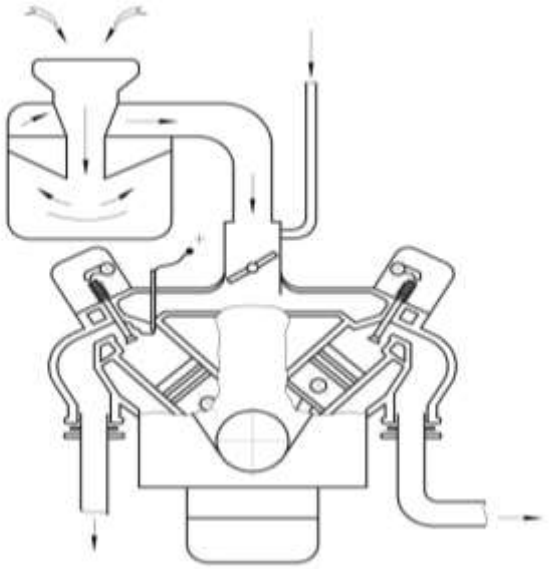

Fig. 2. Scheme of operation of the fuel assembly source

The engine runs at a constant, pre-adjusted crankshaft speed and therefore at a constant performance. Since the intake manifold of the engine is common for all groups of cylinders, the regulation of the mixer performance (crankshaft rotation speed) and the quality of the mixture supplied by the cylinders 5,6,7,8 to the detonation pipe are made by the same engine power system.

Thus, such a source of fuel assemblies will make it possible to obtain a homogeneous fuel blend mixture, which has an increased detonation ability in comparison with a mixture obtained by spraying fuel directly into the air. This is due to the fact that during the compression of the mixture in the engine cylinders, complete evaporation and ideal mixing of fuel with air occur and pre-flame reactions (cold-flame oxidation) occur, accompanied by the formation of organic peroxides, hydrogen peroxide, a significant amount of formaldehyde, etc., facilitating the onset of detonation. ...

Ignition was carried out by a high-voltage discharge on the electrodes of the candle. High voltage pulses were supplied to the spark plug from an initiation system consisting of a 12V power supply (storage battery), an Iskra type ignition unit, an initiating pulse supply control unit, an ignition coil, and a spark plug.

The working body was mounted on special mounting elements in such a way that its outlet nozzle (outer diameter 46 mm, inner diameter 25 mm) was placed vertically at

INNOVATIVE TECHNOLOGICA
METHODICAL RESEARCH JOURNAL
ISSN: 2776-0987 Volume 2, Issue 11, Nov., 2021

a distance of 2-8 cm from the surface of the crust. The crust was formed in special boxes with two transparent walls, as follows:

– The soil was poured into the box and compacted;
– Top-up soil for the crust with a slight compaction;
– Water was poured onto the surface from a watering can from a distance; 0.7 mIm before getting wet 15-20 mm;
– Accelerated soil drying using heating lamps.

In another series of experiments, the soil crust was formed in special shapes to simulate the mechanical properties of the soil. The thickness of the soil crust is 10-20 mm. The need for soil modeling with a soil crust is described below.

The crust was formed on the soil from the fields of the Altyaryk district of the Fergana region.

Experiments on synchronous filming with two cameras of the propagation of a shock wave and the process of soil destruction have shown that the crust destruction visible on the footage occurs 1-1.5 m / s after the wave hits the surface. Therefore, in further experiments, the film recording of the shock wave and the destruction process was carried out separately in independent experiments.

The optical scheme of shooting the shock wave is shown in Fig. 3, where

1-Pulse laser UIG-IM;
2-Outlet tube of the detonation wave generator (GDW);
3-Section of soil with a crust;
4-Shock wave;
5-Frosted glass;
6-Electron-optical camera "Imakon-790".

Figure 4. a functional diagram of a pulsed laser UIG-IM is shown, where:

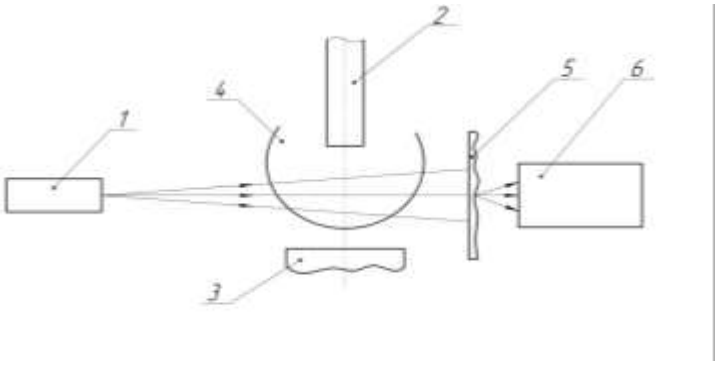

Fig. 3 Optical diagram of the shock wave filming.

INNOVATIVE TECHNOLOGICA
METHODICAL RESEARCH JOURNAL
ISSN: 2776-0987 Volume 2, Issue 11, Nov., 2021

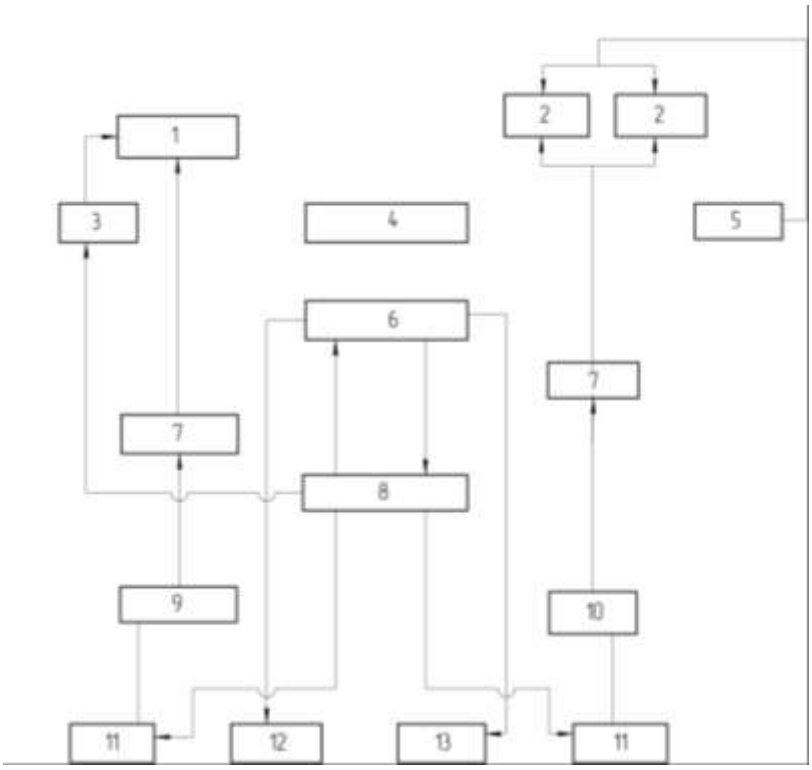

Fig. 4. Functional diagram of a pulsed laser UIG-IM.

1-Illuminator of an optical quantum generator (OCG);
2-Illuminator of optical quantum amplifiers (OQA);
3-Driver ignition 1;
4-Installation holographic;
5-Driver ignition;
6-Control panel;
7-Block of capacitors;
8-Power supply unit;
9-Rectifier block 1;
10-Block rectifier 2;
11-Converter;
12-Cooling system;
13-Auxiliary panel.

INNOVATIVE TECHNOLOGICA
METHODICAL RESEARCH JOURNAL
ISSN: 2776-0987 Volume 2, Issue 11, Nov., 2021

Technical details:

- Radiation wavelength of a laser with a ruby active element, μm	0.6943
- Energy of single-mode laser radiation, J:	
a) Q-switched (monopulse mode)	25 10-3
b) without Q-switching	10-1
- Radiation energy after OKU-1, J:	
a) Q-switched	0.125
b) without Q-switching	0.5
- Radiation energy after OKU-2, J:	
a) Q-switched	0.5
b) without Q-switching	1.5
- The duration of the radiation pulse, s, no more:	
a) Q-switched	4 10-8
b) without Q-switching	4 10-4
- Delay of the radiation pulse relative to the sync pulse, μs	from 5 to 10000
- Time intervals between pulses (with a duration of 40 NS each), μs	from 40 to 250
- Maximum dimensions of the "scene" (when registering on a photographic plate "Mikrat-VR / 2"), mm	
a) section	200x200
b) depth	1000
- Power consumed by the installation from the AC 220 V (50Hz), kW, no more	2
- Overall dimensions of the installation, mm	3500x1300x670
- Unit weight without capacitor banks, kg	200

Analysis of the characteristics of the laser shows that they meet the requirements for shooting an air shock wave of a detonation generator with a propagation velocity of about 10002000 m / s at a distance of up to 10 cm to the surface of the crust.

Electron-optical camera "IMAKON-790".

1. Characteristics of the image-converter. Photocathode 520 with a spectral characteristic extended in the red region; the size of the photocathode is 9 mm x 8 mm; magnification from the cathode to the screen in $2x \pm 0.13$ times.

Screen P_{11} with medium persistence; image size on the screen 16x18 mm at 8 frames; (8x18) mm - at 16 frames; slit image format 18 x 70 mm.

The brightness gain is 50 times per unit area in white light.

INNOVATIVE TECHNOLOGICA
METHODICAL RESEARCH JOURNAL
ISSN: 2776-0987 Volume 2, Issue 11, Nov., 2021

Cathode-screen voltage - 17.5 kV±500 V.

2. Electrical characteristics.

The TI trigger input is designed for a positive voltage pulse from 10 to 200 V with a duration of at least 100 ns and a slew rate of at least IV / ns.

Start input T2 - respectively - 40 200V; not less than 25 ns, not less than 2V/ns.

Power consumption 50V, 100V, 110V, 220V or 240V±10%, 50-60 Hz.

3. Shooting modes:

a) single frame with the number of frames from 8 to 16. Start delay 70ns plus half the interframe interval.

Resolution from 12 pairs / mm at speeds of 10 μs / mm and slower to 9 pairs / mm at 1 ns / mm.

In the region of localization of the shock wave, the gas density is distributed significantly unevenly, which leads to an unequal change in the phases of light rays that have passed through different sections of the optical inhomogeneity (shock wave).

As a result, upon further propagation of the probe wave with a wave front deformed by the inhomogeneity, in accordance with the laws of optics, the light intensity is redistributed in space behind the shock wave. This leads to the formation of an image of the shock wave on the screen located behind the region of its localization. It should be noted that optical inhomogeneity is visualized only when it is illuminated by radiation with a deterministic wavefront, for example, spherical or flat.

This property is possessed by laser radiation in the absence of objects scattering light randomly, such as frosted glass, fog, smoke, etc., on the path of its propagation.

When using thermal (non-laser) light sources for visualization of optical inhomogeneities such as gas-dynamic flows and shock waves, their special preparation in terms of spatial and frequency filtering of radiation is required, which leads to a significant loss of power.

In the diagram in Fig. 3. The radiation of the laser 1 illuminates the shock wave 4, while its image is formed on the frosted glass 5, which is then transferred by the lens of the camera 6 to the photocathode of the electron-optical converter. As a result of the photoeffect, the optical image of the shock wave is converted into an electronic one, and after acceleration and electrostatic focusing of the electron beam on the output luminescent screen (anode), the electronic image is converted back into an optical one and recorded by a contact method on photographic film.

ISSN: 2776-0987 Volume 2, Issue 11, Nov., 2021

Deformation of the crust and the beginning of the formation of visible cracks. The time of the second period is also of the order of 300 μs.

Mass cracking, crust fragmentation, removal of crust particles by gas flow, crater clipping. The time of the third period is of the order of 600 μs (the main crater formation.) It should be noted that the intense removal of small particles from the crater continues throughout the entire process of the outflow of detonation products, up to 0.01 sec.

The size of the crust breakdown is about 50 mm. The micro-fracture zone exceeds the size of the crater and is approximately 120 mm in diameter

References

1. Tojiev, R. J. (2019). Drying glass feed stock in drum drier for manufacturing glass products. Scientific-technical journal, 22(3), 137-140.
2. Isomiddinov, A., Axrorov, A., Karimov, I., & Tojiyev, R. (2019). Application of rotor-filter dusty gas cleaner in industry and identifying its efficiency. Austrian Journal of Technical and Natural Sciences, (9-10).
3. Isomidinov, A. S., Karimov, I. T., & Tojiev, R. J. (2021). Searching the losing of hydraulic pressure in rotor-filter gas cleaner apparatus. Scientific-technical journal, 3(1), 69-72.
4. Ахроров, А. А. У., Исомиддинов, А. С., & Тожиев, Р. Ж. (2020). Гидродинамика поверхностно-контактного элемента ротор-фильтрующего пылеуловителя. Universum: технические науки, (8-3 (77)).
5. Тожиев, Р. Ж., Ахунбаев, А. А., & Миршарипов, Р. Х. (2018). Сушка тонкодисперсных материалов в безуносной роторно-барабанном аппарате. Научно-технический журнал ФерПИ,-Фергана, (2), 116-119.
6. Мўминов, Ж. А., Умаров, Э. С., & Ортиқалиев, Б. С. (2019). Оғир юкланишли ва тез ҳаракатланувчи машина қисмларида сирпаниш подшипникларини танлаш. Машинасозлик ишлаб чиқариш ва таълим: муаммолар ва инновацион ечимлар-2019й, 338-340.
7. Rasuljon, T., Azizbek, I., & Bobojon, O. (2021). Studying the effect of rotor-filter contact element on cleaning efficiency. Universum: технические науки, (6-5 (87)), 28-32.
8. Tojiev, R., Ortikaliyev, B., & Tojiboyev, B. (2019). Improving selecting technology of raw materials of fireproof bricks. Тенденции и перспективы

ISSN: 2776-0987 Volume 2, Issue 11, Nov., 2021

развития науки и оброзования в условиях глобализации. Украина, 27(46), 606-609.
9. Тожиев, Р. Ж., & Ортикалиев, Б. С. (2019). Оловбардош ғишт ишлаб чиқаришда хом ашёларни саралаш жараёнини тадқиқ қилиш. Журнал Технических исследований, (2).
10.Ахунбаев, А., Ражабова, Н., & Вохидова, Н. (2021). Механизм движения дисперсного материала при сушке тонкодисперсных материалов. Збірник наукових праць SCIENTIA.
11.Tojiyev, R. J., Ortiqaliyev, B. S. O. G. L., Abdupattoyev, X. V. O., & Isomiddinova, D. I. J. Q. (2021). Donador-sochiluvchan mahsulotlarni saralashda sm-237a markali mashinalarini o‘rni. Scientific progress, 2(2), 1378-1381.
12.Ортикалиев, Б. С., & Тожиев, Р. Ж. Оловбардош гишт ишлаб чикаришда хом ашёларни саралаш жараёнини тадкик килиш. Техник тадкикотлар журнали-2019 й.
13.Tojiyev, R., Ortiqaliyev, B., & Sotvoldiyev, K. (2021). Improving the design of the screed for firebricks using solidworks. Барқарорлик ва Етакчи Тадқиқотлар онлайн илмий журнали, 1(5), 91-99.
14.Ахунбаев, А., Ражабова, Н., & Сиддиков, М. (2021). Математическая модель сушки дисперсных материалов с учётом температуры материала. Збірник наукових праць SCIENTIA.
15.Ортиқалиев, Б. С., and Р. Ж. Тожиев. "Sifatli olovbardosh g ‘isht ishlab chiqarishda xom ashyolarni saralash jarayonini tadqiq qilish." Замонавий бино–иншоотларни ва уларнинг конструкцияларини (2021).
16.Ахунбаев, А. А., Ражабова, Н. Р., & Вохидова, Н. Х. (2020). Исследование гидродинамики роторной сушилки с быстровращающимся ротором. Экономика и социум, (12-1), 392-396.
17.Ахунбаев, А. А., & Ражабова, Н. Р. (2021). Высушивание дисперсных материалов в аппарате с быстро вращающимся ротором. Universum: технические науки, (7-1 (88)), 49-52.
18.Тожиев, Р. Ж., Исомиддинов, А. С., Ахроров, А. А. У., & Сулаймонов, А. М. (2021). Выбор оптимального абсорбента для очистки водородно-фтористого газа в роторно-фильтровальном аппарате и исследование эффективности аппарата. Universum: технические науки, (3-4 (84)), 44-51.

ISSN: 2776-0987 Volume 2, Issue 11, Nov., 2021

19.Rasuljon, T., Azizbek, I., & Abdurakhmon, S. (2021). Research of the hydraulic resistance of the inertial scrubber. Universum: технические науки, (7-3 (88)), 44-51.
20.Mukhamadsadikov, K. J., & ugli Ortikaliev, B. S. (2021). Working width and speed of the harrow depending on soil resistivity. Web of Scientist: International Scientific Research Journal, 2(04), 152-158.